Thin Solid Films 582 (2015) 162–165

Contents lists available at ScienceDirect

Thin Solid Films

journal homepage: www.elsevier.com/locate/tsf

Temperature dependent current transport properties in Cu_2ZnSnS_4 solar cells

Mati Danilson [a,*], Erkki Kask [b], Nikhil Pokharel [a,c], Maarja Grossberg [a], Marit Kauk-Kuusik [a], Tiit Varema [a], Jüri Krustok [a,b]

[a] Department of Materials Science, Tallinn University of Technology, Ehitajate tee 5, 19086 Tallinn, Estonia
[b] Department of Physics, Tallinn University of Technology, Ehitajate tee 5, 19086 Tallinn, Estonia
[c] Department of Natural Sciences (Physics), Kathmandu University, PO Box 6250 Dhulikhel, Nepal

ARTICLE INFO

Available online 25 October 2014

Keywords:
Copper zinc tin sulfide
Solar cells
Temperature effect
Current transport
Serial resistance
Quantum efficiency
Current–voltage characteristics
Impedance spectroscopy

ABSTRACT

Quaternary semiconductor compound Cu_2ZnSnS_4 (CZTS) is a promising non-toxic absorber material for solar cells made from earth abundant elements. In this study temperature dependencies (T = 10–300 K) of current–voltage (J–V) characteristics and external quantum efficiency (EQE) spectra of CZTS monograin layer solar cells were measured in order to clarify current transport in CZTS that is still not fully understood. Three different temperature ranges can be distinguished from the temperature dependence of the series resistance (R_s) obtained from J–V measurements and the effective bandgap energy (E_g^*) determined from the EQE spectra. Thermally activated conductivity, Mott's variable-range hopping conductivity, and very low temperature (<40 K) blocking of the interface recombination were observed.

© 2014 Elsevier B.V. All rights reserved.

1. Introduction

Multinary semiconductor compounds $Cu_2ZnSn(Se_xS_{1-x})_4$ (CZTSSe) are promising non-toxic absorber materials for solar cells made from earth abundant elements. Currently, the power conversion efficiency record of Cu_2ZnSnS_4 (CZTS) device is 8.4% [1] and that of CZTSSe device — 12.6% [2]. High series resistance and interface recombination are reported as the main limiting factors in CZTS-based solar cells [3,4]. Hence, almost all basic solar cell parameters are limited by recombination and parasitic losses. Moreover, most of CZTS absorbers used in solar cells show properties of so-called heavily doped semiconductors, where high concentration of charged defects leads to a formation of spatial potential fluctuations [5]. Accordingly, different type of current transport and recombination mechanisms can be observed [6–9].

In CZTS solar cells recombination losses are not only related to the interface between absorber and buffer layers but also to different bulk defects or band tails. The first-principle calculations have been made for CZTS by Chen et al. [10]. They found that the main acceptor defect in CZTS is Cu_{Zn} antisite defect that has a quite deep level at E_A = 0.12 eV. This acceptor was also found by admittance spectroscopy [11]. Even deeper acceptor (E_A = 0.28 eV) was detected in CZTS by photoluminescence spectroscopy [12]. These quite deep defects can be efficient recombination centers even at temperatures close to room temperature. At the same time, Chen et al. [13] have shown that the compensation between the dominant acceptor defect Cu_{Zn} and the donor defect Sn_{Zn} can significantly decrease the formation energies of the defect clusters (Cu_{Zn} + Sn_{Zn} and $2Cu_{Zn}$ + Sn_{Zn}) leading to high concentrations of these clusters even in stoichiometric samples. It was shown that the recombination through these defect clusters dominates in most CZTS samples at low temperatures [14]. The presence of different defect complexes in CZTS was also proposed by Huang et al. [15]. According to their calculations these complexes can cause a significant local band gap decrease and boost the recombination.

The temperature-dependent conductivity of polycrystalline CZTS thin films [3,4,6–9] and single crystals [16] has been studied in many papers. However, in real solar cell structures many different recombination channels appear which are not present in bulk CZTS. Therefore, it is extremely interesting to study temperature dependence of these real structures. We already have studied the temperature dependencies of $Cu_2ZnSnSe_4$ monograin layer (MGL) solar cells and showed how potential fluctuations change the current transport in these structures [17]. In this study, current–voltage (J–V) characteristics and external quantum efficiency (EQE) curves were used for characterizing recombination and parasitic effects in order to identify loss mechanisms and reveal current transport properties in CZTS-based MGL solar cells.

* Corresponding author at: Ehitajate tee 5, 19086, Tallinn, Estonia. Tel.: +372 6203210; fax: +372 6203367.
E-mail addresses: mati.danilson@ttu.ee (M. Danilson), erkki.kask@ttu.ee (E. Kask), pokharel.nikhil@gmail.com (N. Pokharel), Maarja.Grossberg@ttu.ee (M. Grossberg), marit.kauk-kuusik@ttu.ee (M. Kauk-Kuusik), Tiit.Varema@ttu.ee (T. Varema), juri.krustok@ttu.ee (J. Krustok).

http://dx.doi.org/10.1016/j.tsf.2014.10.069
0040-6090/© 2014 Elsevier B.V. All rights reserved.

2. Experimental

CZTS monograins were synthesized from binaries and elemental S in molten flux by isothermal recrystallization process. The details of the monograin growth technology can be found elsewhere [18]. MGL solar cells with structure: graphite/MGL/CdS/ZnO/glass, were made from powder crystals with a diameter of 56–63 μm as selected by sieving. The analysis area of the solar cell is determined by the back contact area which is typically about 0.04 cm^2. More details about the solar cell preparation can be found in [19].

For the temperature dependent J–V and EQE measurements solar cells were mounted in a closed cycle He cryostat. J–V measurements were done by decreasing the temperature while EQE measurements were done by increasing the temperature in the range $T = 10$–300 K. For EQE measurements the generated photocurrent was detected at 0 V bias voltage. 250 W standard halogen lamp with calibrated intensity (100 mW cm^{-2}) was used as a light source and spectrally neutral net filters for intensity dependence.

3. Results and discussion

Room temperature J–V characteristics of a studied CZTS-based MGL solar cell showed the following properties: open-circuit voltage $V_{oc} =$ 709 mV, short-circuit current density $J_{sc} = 13.8$ mA/cm^2, fill factor $FF = 61.4\%$, and efficiency $\eta = 6.0\%$. Due to the peculiarity of the MGL solar cell structure, the active area where the photocurrent is actually produced is smaller than the analysis area. The active area is estimated to be 75% of the back contact area after excluding the area of the binder material between the absorber material powder crystals. After such consideration the current density per absorber material active area is estimated to be $J_{sc}^{abs.} = 18.4$ mA/cm^2 and the efficiency is estimated to be $\eta^{abs} = 8.0\%$. In spite of that, solar cell parameters are still limited due to recombination and parasitic losses. The series resistances obtained from the light and the dark J–V curves determined at room temperature by the process described by Hegedus and Shafarman [20] are rather high, $R_s^{light} = 3.6\ \Omega\ cm^2$ and $R_s^{dark} = 4.5\ \Omega\ cm^2$, accordingly.

The thermal behavior of the V_{oc} under different light intensities is shown in Fig. 1. It is known [21] that the temperature dependence of V_{oc} near room temperature can be presented as

$$V_{OC} = \frac{E_A}{q} - \frac{nkT}{q} \ln\left[\frac{I_{00}}{I_L}\right], \tag{1}$$

where E_A, n, k, I_{00}, and I_L are the activation energy, diode ideality factor, Boltzmann constant, reverse saturation current prefactor, and the photocurrent, respectively. In general, the activation energy E_A and also I_{00} depend mainly on the dominating recombination mechanism in the solar cell. In case of bulk recombination $E_A \approx E_g$, where E_g is the bandgap energy of the absorber material. The bandgap energy of CZTS slightly depends on the type of crystal structure [12], but is usually higher than 1.5 eV. In our sample $E_A \approx 1.26$ eV was determined from the V_{oc} (T) plot (see Fig. 1). In general, according to the theory [22] in case of $E_A < E_g$, the interface recombination is a dominating recombination.

The temperature dependence of the series resistance R_s found using Fig. 2 is shown in Fig. 3a where three different regions can be distinguished. At temperatures $T > 90$ K (region I) R_s decreases with increasing temperature indicating the thermal activation of carriers [23]. In this region, the R_s can be presented as:

$$R_S = R_{S0} \exp(E_A/kT) \tag{2}$$

where the exponential prefactor R_{S0} contains all parameters that are independent or weekly dependent on temperature. Using Eq. (2) the activation energies $E_{A,d} = 87 \pm 3$ meV and $E_{A,l} = 43 \pm 1$ meV for dark and light curves were found, respectively. These activation energies are in the same range as found in [6,8,24]. At intermediate temperatures ($T = 90$–40 K, region II), the dependence of the series resistance on temperature changes and a typical Mott's variable-range hopping (VRH) conduction starts to dominate [25]. This type of behavior is expected in all heavily doped materials where spatial potential fluctuations create deep potential wells for holes [6,26,27]. At the same time, we also expect the increasing role of bulk recombination in this temperature region and therefore the VRH model is not completely valid here. At about $T = 40$ K, a rapid change of R_s can be seen. In low temperature region ($T < 40$ K, region III), R_s drops down more than one order of magnitude and remains almost constant down to the lowest measured temperature. At these very low temperatures, generated holes are not able to tunnel through the potential barrier into the interface region between CZTS and CdS and therefore the interface recombination rate must be very low.

Quantum efficiency measurement is a well-known method to describe optical and electronic losses in solar cell devices. From the low-energy side of the EQE curve i.e. near the bandgap energy $E \approx E_g$, the effective bandgap energy E_g^* can be determined [17] by using an approximation proposed by Klenk and Schock [28]:

$$EQE \approx K\alpha L_{eff} \approx A\left(E - E_g^*\right)^{1/2}/E \tag{3}$$

where constant A includes all energy independent parameters, $L_{eff} = w + L_d$ is the effective diffusion length of minority carriers, L_d is their diffusion length in the absorber material, w is the width of the depletion region, and α is the absorption coefficient of the absorber material. The constant K is unity in absolute measurements. Consequently, the E_g^* value can be determined from a plot of

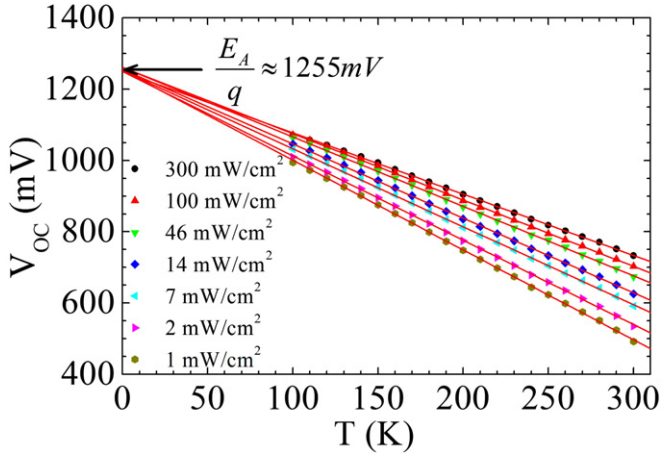

Fig. 1. Temperature dependence of V_{oc} measured at different light intensities.

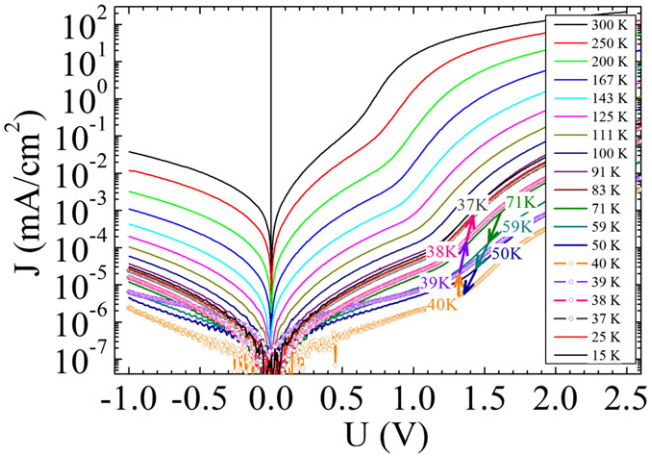

Fig. 2. Temperature dependence of dark J–V curves.

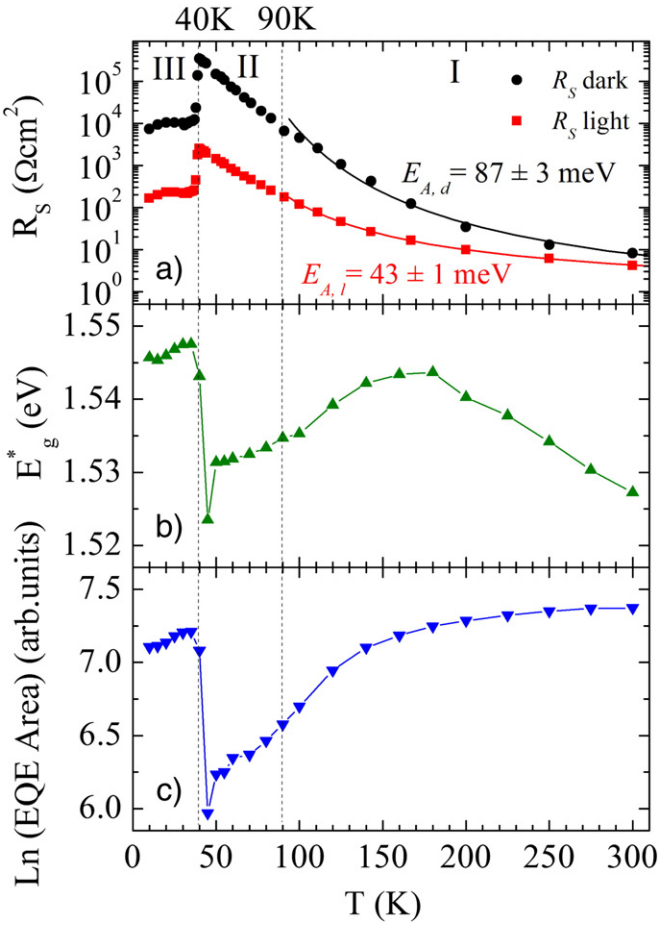

Fig. 3. Temperature dependencies of the series resistance R_s obtained from the dark and light J–V curves (a), the effective bandgap energy E_g^* (b), and integrated EQE area (c). Solid lines correspond to the fitting of Eq. (3) to the experimental data.

$(E \cdot EQE)^2$ vs. E at the low energy side of the EQE spectrum. Therefore, temperature dependence of a quantum efficiency curve presented in Fig. 4 can be used to analyze the temperature dependence of the effective bandgap energy.

The temperature dependencies of the series resistance R_S, the effective bandgap energy E_g^* and the integrated EQE are presented in Fig. 3. It can be seen (Fig. 3b) that in the temperature region from room temperature to $T = 180$ K, E_g^* follows the model of temperature dependence of the bandgap energy proposed by K.P. O'Donnell and X. Chen [29]. Then E_g^* starts to decrease with further decreasing of the temperature until the "critical" temperature at about 40 K where the rapid increase of E_g^* starts. Similar behavior can be seen for integrated EQE, see Fig. 3c. It was shown in [17] that the changes at 40 K < T < 180 K are related to localization of holes inside deep valence band potential wells. As a result, an exponential Urbach tail starts to affect the absorption and the effective bandgap E_g^* starts to decrease due to holes localization in deeper potential wells. At the same time the hole mobility also decreases and the bulk recombination through these deep wells increases reducing the overall EQE. The observed sudden increase of E_g^* to the "normal" bandgap value E_g at 40 K together with the increase of the generated current (EQE) and decrease in R_s has to be related to the step-like change in the Fermi level position at the interface. This change could cause the blocking of hole transport to the interface states and as a result the interface recombination decreases. This is why the photocurrent and E_g^* increase. However, there might be also other processes taking place causing the same kind of behavior. Consequently further studies are needed to explain this peculiar behavior of the CZTS solar cell parameters at very low temperatures.

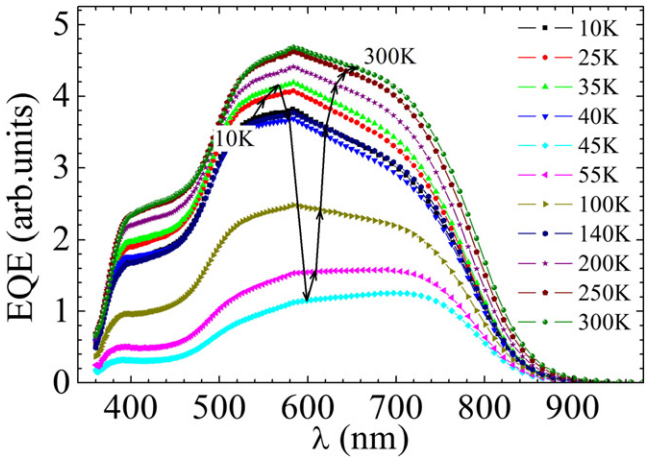

Fig. 4. Temperature dependence of EQE at 0 V. The arrows guide the trend of the EQE temperature dependence.

4. Conclusions

Temperature dependence of CZTS solar cell parameters was measured in the range of T = 10–300 K. It was shown that main recombination losses are related to interface recombination that was found to be blocked at T < 40 K. Part of the losses originate also from bulk recombination and is associated to potential fluctuations of the valence band edge.

Acknowledgments

This work was supported by the Estonian Science Foundation grants ETF 9369, ETF 9425, and ETF 9346, by the institutional research funding IUT 19-28 of the Estonian Ministry of Education and Research, Estonian Centre of Excellence in Research, Project TK117, National R&D program "Energy", Project AR10128, and by the Estonian Material Technology Programme, Project AR12128. This paper was also supported by the national scholarship program Kristjan Jaak, grand number 16-3.3/351, which is funded and managed by Archimedes Foundation in collaboration with the Ministry of Education and Research.

References

[1] B. Shin, O. Gunawan, Y. Zhu, N.A. Bojarczuk, S.J. Chey, S. Guha, Thin film solar cell with 8.4% power conversion efficiency using an earth-abundant Cu_2ZnSnS_4 absorber, Prog. Photovolt. Res. Appl. 21 (2013) 72.
[2] W. Wang, M.T. Winkler, O. Gunawan, T. Gokmen, T.K. Todorov, Y. Zhu, D.B. Mitzi, Device characteristics of CZTSSe thin-film solar cells with 12.6% efficiency, Adv. Energy Mater. 4 (2013) 1301465.
[3] K. Wang, O. Gunawan, T. Todorov, B. Shin, S.J. Chey, N.A. Bojarczuk, D. Mitzi, S. Guha, Thermally evaporated Cu_2ZnSnS_4 solar cells, Appl. Phys. Lett. 97 (2010) 143508.
[4] O. Gunawan, T. Todorov, D. Mitzi, Loss mechanisms in hydrazine-processed Cu2ZnSn(Se, S)4 solar cells, Appl. Phys. Lett. 97 (2010) 233506.
[5] M. Grossberg, P. Salu, J. Raudoja, J. Krustok, Microphotoluminescence study of Cu_2ZnSnS_4 polycrystals, J. Photonics Energy 3 (2013) 030599.
[6] V. Kosyak, M.A. Karmarkar, M.A. Scarpulla, Temperature dependent conductivity of polycrystalline Cu_2ZnSnS_4 thin films, Appl. Phys. Lett. 100 (2012) 263903.
[7] M.A. Majeed Khan, S. Kumar, M. Alhoshan, A.S. Al Dwayyan, Spray pyrolysed Cu_2ZnSnS_4 absorbing layer: a potential candidate for photovoltaic applications, Opt. Laser Technol. 49 (2013) 196.
[8] J.C. González, G.M. Ribeiro, E.R. Viana, P.A. Fernandes, P.M.P. Salomé, K. Gutiérrez, A. Abelenda, F.M. Matinaga, J.P. Leitão, A.F. da Cunha, Hopping conduction and persistent photoconductivity in Cu_2ZnSnS_4 thin films, J. Phys. D. Appl. Phys. 46 (2013) 155107.
[9] M. Guc, R. Caballero, K.G. Lisunov, N. López, E. Arushanov, J.M. Merino, M. León, Disorder and variable-range hopping conductivity in Cu_2ZnSnS_4 thin films prepared by flash evaporation and post-thermal treatment, J. Alloys Compd. 596 (2014) 140.
[10] S. Chen, J.-H. Yang, X.G. Gong, A. Walsh, S.-H. Wei, Intrinsic point defects and complexes in the quaternary kesterite semiconductor Cu_2ZnSnS_4, Phys. Rev. B 81 (2010) 245204.

[11] E. Kask, T. Raadik, M. Grossberg, R. Josepson, J. Krustok, Deep defects in Cu_2ZnSnS_4 monograin solar cells, Energy Procedia 10 (2011) 261.
[12] M. Grossberg, J. Krustok, J. Raudoja, T. Raadik, The role of structural properties on deep defect states in Cu_2ZnSnS_4 studied by photoluminescence spectroscopy, Appl. Phys. Lett. 101 (2012) 102102.
[13] S. Chen, L.-W. Wang, A. Walsh, X.G. Gong, S.-H. Wei, Abundance of $Cu_{Zn} + Sn_{Zn}$ and $2Cu_{Zn} + Sn_{Zn}$ defect clusters in kesterite solar cells, Appl. Phys. Lett. 101 (2012) 223901.
[14] M. Grossberg, T. Raadik, J. Raudoja, J. Krustok, Photoluminescence study of defect clusters in Cu_2ZnSnS_4 polycrystals, Curr. Appl. Phys. 14 (2014) 447.
[15] D. Huang, C. Persson, Band gap change induced by defect complexes in Cu_2ZnSnS_4, Thin Solid Films 535 (2013) 265.
[16] K.G. Lisunov, M. Guk, A. Nateprov, S. Levcenko, V. Tezlevan, E. Arushanov, Features of the acceptor band and properties of localized carriers from studies of the variable-range hopping conduction in single crystals of p-Cu_2ZnSnS_4, Sol. Energy Mater. Sol. Cells 112 (2013) 127.
[17] J. Krustok, R. Josepson, T. Raadik, M. Danilson, Potential fluctuations in $Cu_2ZnSnSe_4$ solar cells studied by temperature dependence of quantum efficiency curves, Physica B 405 (2010) 3186.
[18] K. Muska, M. Kauk, M. Grossberg, J. Raudoja, O. Volobujeva, Influence of compositional deviations on the properties of $Cu_2ZnSnSe_4$ monograin powders, Energy Procedia 10 (2011) 323.
[19] K. Muska, M. Kauk-Kuusik, M. Grossberg, M. Altosaar, M. Pilvet, T. Varema, K. Timmo, O. Volobujeva, A. Mere, Impact of $Cu_2ZnSn(Se_xS_{1-x})_4$ ($x = 0.3$) compositional ratios on the monograin powder properties and solar cells, Thin Solid Films 535 (2013) 35.
[20] S.S. Hegedus, W.N. Shafarman, Thin-film solar cells: device measurements and analysis, Prog. Photovolt. Res. Appl. 12 (2004) 155.
[21] J. Krustok, R. Josepson, M. Danilson, D. Meissner, Temperature dependence of $Cu_2ZnSn(Se_xS_{1-x})_4$ monograin solar cells, Sol. Energy 84 (2010) 379.
[22] V. Nadenau, U. Rau, A. Jasenek, H.W. Schock, Electronic properties of $CuGaSe_2$-based heterojunction solar cells. Part I. Transport analysis, J. Appl. Phys. 87 (2000) 584.
[23] J.T. Asubar, Y. Jinbo, N. Uchitomi, Impurity band conduction and negative magnetoresistance in p-$ZnSnAs_2$ thin films, Phys. Status Solidi C 6 (2009) 1158.
[24] P.A. Fernandes, P.M.P. Salome, A.F. Sartori, J. Malaquias, A.F. da Cunha, B.-A. Schubert, J.C. González, G.M. Ribeiro, Effects of sulphurization time on Cu_2ZnSnS_4 absorbers and thin films solar cells obtained from metallic precursors, Sol. Energy Mater. Sol. Cells 115 (2013) 157.
[25] N.F. Mott, Impurity band conduction. Experiment and theory. The metal–insulator transition in an impurity band, J. Phys. Colloques 37 (1976) C4.
[26] S. Siebentritt, N. Papathanasiou, M.Ch. Lux-Steiner, Potential fluctuations in compensated chalcopyrites, Physica B 831 (2006) 376.
[27] M. Grossberg, J. Krustok, J. Raudoja, K. Timmo, M. Altosaar, T. Raadik, Photoluminescence and Raman study of $Cu_2ZnSn(Se_xS_{1-x})_4$ monograins for photovoltaic applications, Thin Solid Films 519 (2011) 7403.
[28] R. Klenk, H.-W. Schock, W.H. Bloss, Photocurrent collection in thin film solar cells — calculation and characterization for CuGaSe2/(Zn,Cd)S, Proc. of the 12th EU PVSEC, 1994, p. 1588.
[29] K.P. O'Donnell, X. Chen, Temperature dependence of semiconductor band gaps, Appl. Phys. Lett. 58 (1991) 2924.